Hyper-viscoelastic Response of Perfused Liver under Dynamic Compression and Estimation of Tissue Strain Thresholds with a Liver Finite Element Model

Fusako Sato , Yoshihiro Yamamoto, Daisuke Ito, Jacobo Antona-Makoshi, Susumu Ejima,
Koichi Kamiji, Tsuyoshi Yasuki

Abstract A liver Finite Element (FE) model with hyper-viscoelastic properties was developed. Hyper-elastic and rate-dependent characteristics were modeled with an Ogden rubber material model. Such characteristics were validated against an original series of porcine exsanguinated livers under quasi-static and dynamic compression experiments. The applicability of the validated liver FE model was evaluated against a series of compression tests with porcine perfused livers to model nearly in vivo conditions. The regions where the FE model showed highest strain concentrations corresponded with the regions where perfused livers tested under dynamic loading sustained tissue damage. Based on this correspondence, ultimate strains for hepatic parenchyma and membrane were estimated by comparing strain patterns of the FE model with damaged conditions of the tested livers.

Keywords inner organ injury, finite element model, liver, liver compression test, tissue strain threshold

I. INTRODUCTION

The liver is the most frequently injured abdominal organ in front and side impact vehicle crashes [1-2]. In such crashes, occupants are subjected to dynamic loadings that are transferred to the abdominal region, causing large deformations of the liver tissue. However, many aspects of the liver injury mechanisms are still unknown and further research to clarify them is needed. For this purpose, human body Finite Element (FE) models can be utilized, but reliable injury simulations demand valid organ models. Characterization of the tissue properties, simulation of the behaviour of the whole liver under various loading conditions and establishment of injury thresholds are three important steps in this direction. Thereafter, once sufficient reliability of the models is achieved, the motion of the inner organ of the body and its interaction with other organs under vehicle crash conditions will need to be assessed and validated by experiments [3] and through mathematical simulations.

Stress-strain response of in-vivo perfused livers is non-linear for all compression rates and the tissue response stiffens as the loading speed increases, indicating strong rate-dependence [4]. In line with this behavior, previous numerical studies considered such non-linear and rate-dependent characteristics of the liver. In these studies, the elastic behavior of the liver was commonly modeled with hyper-elastic formulation based on experimental data with small sample pieces of the liver under quasi-static loading conditions [5-10]. Dynamic mechanical response of the liver is also important to simulate impact events and a few studies conducted high-strain-rate testing with small liver pieces [11-13]. The dependency of liver behavior on deformation rate was also tested with small liver pieces and modeled through viscoelasticity [14]. Once a whole liver FE model is built up, the response of the model must be validated against whole liver level experimental data. Furthermore, in order to be able to predict injuries, physical variables, such as stress or strain, and their associated thresholds must also be validated based on whole liver injurious experimental data.

In addition, other aspects need to be considered in modeling the liver of living subjects in order to be integrated in full-scale human FE models. Under living conditions, the liver is filled with blood, which affects its ability to resist external loading [15-18] and increases the difficulties to build reliable models. Some numerical studies considered the behaviour of perfused porcine liver at relatively low strain rate and the dynamic behaviour of the in-vivo perfused monkey liver test [4] with hyper-viscoelasticity [19-21]. However, there are

F. Sato is a researcher at the Japan Automobile Research institute (JARI), Japan (Ph: +81-29-856-0885, fsatou@jari.or.jp). Y. Yamamoto, D. Ito and J. Antona-Makoshi are reseachers at JARI. S. Ejima is the research manager at JARI. K. Kamiji and T. Yasuki are members of the Japan Automobile Manufacturers Association (JAMA), Japan.

difficulties to obtain failure properties of the perfused liver experimentally; there is still a lack of the thresholds of physical variables to predict injuries under perfused conditions.

The ultimate goal of this research is to reduce abdominal injuries in traffic accidents. For this, we provide a validated liver FE model and liver tissue injury strain thresholds to be applied in human models for improved vehicle safety. These model and thresholds, when properly used, can lead to the clarification of liver injury mechanisms and support the deployment of effective countermeasures to achieve the reductions of abdominal injuries.

The specific aims of this study are as follows:

1) Develop a liver FE model with hyper-elastic and viscoelastic characteristics,
2) Validate the response and injury thresholds of the liver FE model,
3) Investigate the applicability of the liver FE model in simulating perfused liver conditions, and
4) Estimate liver tissue strain thresholds applicable for modeling under nearly in vivo conditions.

II. METHODS

A multi-stage inverse methodology was applied to develop and validate the liver FE model in parallel with the execution of four original series of compression tests with porcine liver specimens. The porcine liver was used as a surrogate to the human liver due to similarities in structure and function with the human liver [22]. Exsanguinated and fluid-perfused specimens for both quasi-static and dynamic-loading conditions were employed. All the experimental series were conducted at Niigata University laboratories with specimens purchased from a local slaughter house [23-25]. The specimens were extracted within three hours after sacrifice and transported to the laboratory and kept in saline solution at room temperature until testing. All tests were conducted within 12 hours after death.

A scheme of the experimental series is shown in Figure 1. From the experiments, force displacement curves were obtained and used to define and validate the material properties of the liver FE model at different stages. The working methodology is sketched in Figure 2.

The non-linear and rate-dependent material properties of the liver FE model were defined based on the tests under exsanguinated conditions. In doing so, a two-step approach was applied to account for both the hyper-elastic and the viscoelastic behaviors (Steps 2 & 3). These material characteristics were implemented in the FE model and validated against a series of porcine liver quasi-static and dynamic tests, respectively (Test Series 1 & 2). In addition, liver tissue thresholds for ultimate strain from the literature were implemented in the model and validated against the comparison between the liver FE model and damage conditions of the tested livers (Step 4).

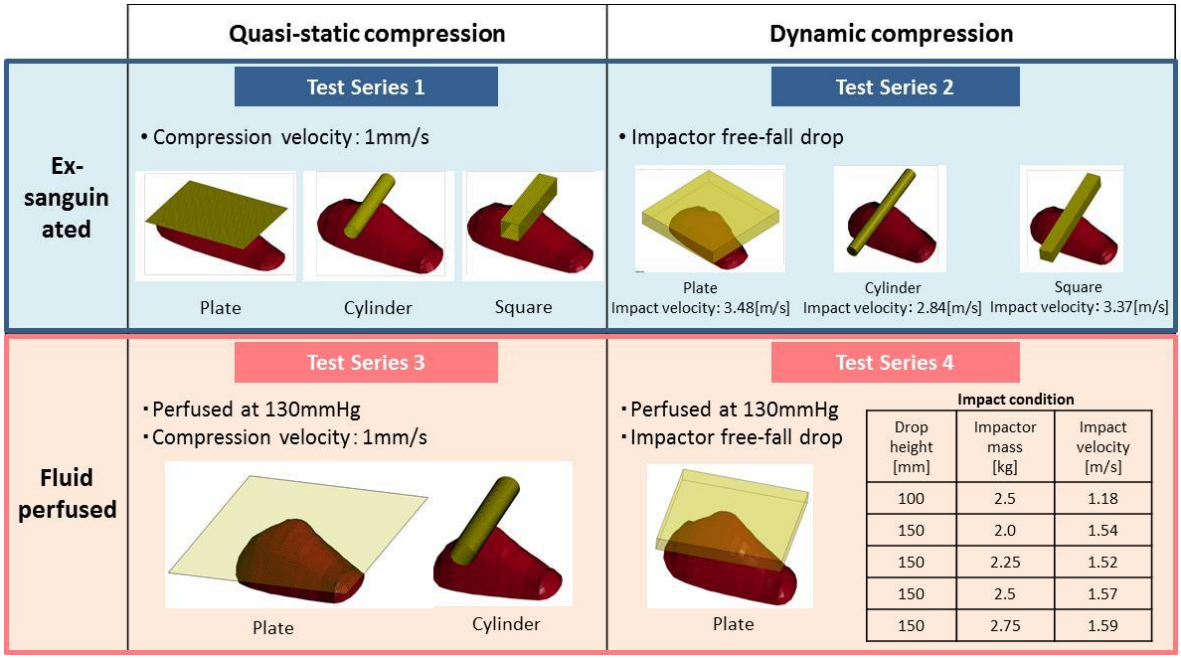

Fig. 1.Scheme of liver compression test series carried out in this study

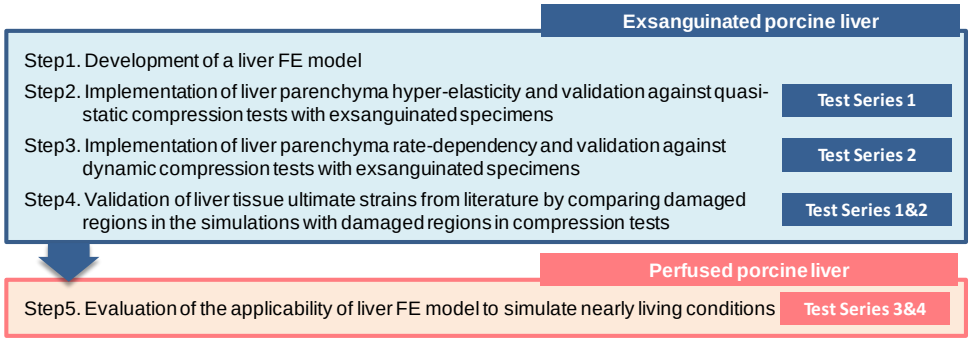

Fig. 2. Multi-step FE model development and validation process

Finally, the applicability of the validated liver FE model was evaluated against two series of porcine liver compression tests at quasi-static and dynamic conditions, respectively (Test Series 3 & 4, Step 5). In these series, the specimens were perfused with a constant flow of fluid to approximate in vivo conditions. By simulating these experiments and comparing the strain patterns from the simulations with the damaged conditions of the tested livers, ultimate strain values to be used for liver FE models under approximately in vivo conditions could be defined.

Step 1. Development of a Liver FE Model

A liver FE model was developed based on three-dimensional geometric data from the right lateral lobe of the exanguinated porcine liver specimens employed in the compression experiments [23-25]. A mesh of the parenchyma was built with approximately 2 mm size hexahedral elements. The hepatic membrane which covers the liver was modeled with membrane elements of 0.045 mm thickness based on a previous study [26]. Hepatic membrane material properties are non-linear [27]. However, in order to ensure numerical stability at high speed impacts, the material properties of the hepatic membrane model were defined as linear elastic with Young's modulus of 34 MPa and Poisson ratio of 0.49, according to tensile tests [23]. All the simulations in this study were conducted using a commercial FE solver LS-DYNA.

Step 2. Implementation of liver parenchyma hyper-elasticity and validation against quasi-static compression tests with exsanguinated specimens

Definition of material properties

The fundamental stress-strain curves of liver parenchyma were defined based on quasi-static uni-axial tension-compression tests with small samples of porcine liver tissue in previous reports [5][7][8][10][13][14]. The stress-strain curve obtained by Sakuma [8] was chosen because the tests were conducted at strain rates of approximately 0.03s-1, which is consistent with the approximated strain rate estimated by the compression ratio rate employed in the whole liver compression tests in this study [24]. Furthermore, Sakuma conducted tension and compression tests continuously. The experiment showed different properties in tension and compression and it is necessary to consider both types of tissue properties in the liver FE model.

The stress-strain curves by Sakuma were highly non-linear and contained no linear portion from which a meaningful elastic modulus could be determined. As the magnitude of the strain increases, the material behaves more stiffly. Based on the curvature, the elastic behavior of the liver was modeled as hyper-elasticity. A hyper-elastic material is defined based on strain energy potential, W. The strain energy formulation utilized in this study is of the Ogden form [29] given by equation (1):

$$\mathbf{W}^{*} = \sum_{\mathbf{i=1}}^{\mathbf{3}} \sum_{\mathbf{j=1}}^{\mathbf{3}} \frac{\mu_j}{\alpha_j}\left(\lambda_i^{*\alpha_j} - \mathbf{1}\right) + \mathbf{K(J - 1 - lnJ)} \quad (1)$$

where λ_i^{*} ($i = 1,2,3$) is principal stretch ratio ((*) indicates that the volumetric effects have been eliminated from the principal stretch ratios). K is bulk modulus, J is relative volume, and μ and α are material constants determined by fitting to an experimental stress-strain curve. The required order of the formulation, designated by n, is determined empirically to obtain a sufficiently accurate fit. A Poisson ratio of 0.499 was defined for the material model, based on the assumption that solid abdominal organs are nearly incompressible [30-31]. Figure 3 shows Sakuma's stress–stretch ratio experimental curve and the fitted Ogden material model curve, the parameters of which are listed in Table I.

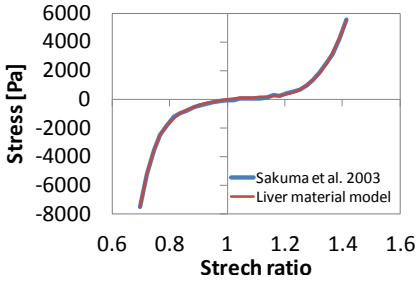

Fig. 3. Stress-Stretch ratio curve for hyper-elastic properties

TABLE I
Ogden parameters

i	μ_i [Pa]	α_i [-]
1	3.7244E+04	5.5872E+00
2	-1.5281E+05	3.5132E+00
3	-3.3660E+05	2.0948E+00
4	3.5137E+06	7.3096E-01
5	2.7666E+06	-7.4234E-01
6	-2.2088E+05	-2.3587E+00

Validation of the liver FE model

The FE model with the hyper-elastic characteristics was validated against a series of quasi-static compression tests using exsanguinated whole porcine livers with three types of impactors: plate, cylinder and square [23] (Test Series 1 in Figure 1). In this series, a total of 16 liver samples (5 for the plate, 5 for the cylinder and 6 for the square) were subjected to quasi-static load at a velocity of 1 mm/s up to 60% compression ratio of the initial height by using a universal testing machine (AUTOGRAPH, Shimadzu, Kyoto, Japan) (Figure 4, Figure 5, Figure 6).

A porcine liver has four regions-right medial, right lateral, left medial and left lateral lobes (Figure 7). Each of these sections was taken apart and tested as an isolated specimen. No significant differences on load-displacement curve and yield loads were observed among the four porcine liver regions [23]. Therefore the liver FE model described in Step 1 was used unalterably to simulate each group of tests. A rigid model for each of the impactors was built and utilized together with the liver FE model. The results of the simulations were compared with the experimental measurements in terms of force versus compression ratio.

(a) Plate 300 x 300 x 30 mm (b) Cylinder ϕ25 x 250 mm (c) Square 30 x 30 x 250 mm

Fig. 4. Impactors used for the quasi-static compression tests

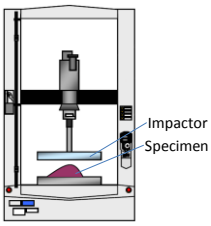

Fig. 5. Illustration of the quasi-static compression testing

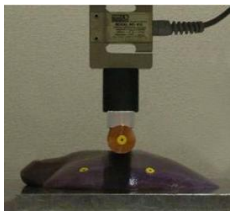

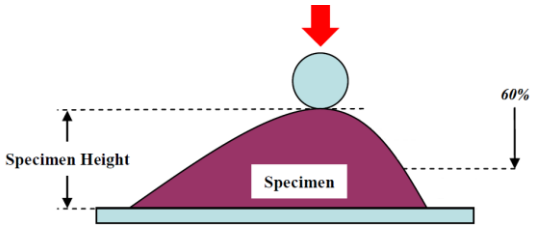

Fig. 6. Definition of compression ratio

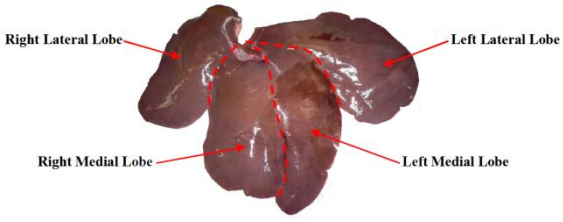

Fig. 7. A porcine liver specimen

Step 3. Implementation of liver parenchyma rate-dependency and validation against dynamic compression tests with exsanguinated specimens

Definition of material properties

Liver tissue response stiffens as the loading speed increases, indicating strong strain rate dependence [4]. In order to capture the rate-dependent effects, a viscoelastic component was modeled and superimposed linearly onto the hyper-elastic formulation previously described in a similar way to that proposed in the literature [20] [21] [32]. The

rate effects were taken into account through linear viscoelasticity given by equation (2):

$$\sigma_{ij} = \int_0^t g_{ijkl}(t-\tau)\frac{\partial \varepsilon_{kl}}{\partial \tau}d\tau \quad (2)$$

where $g_{ijkl}(t-\tau)$ is the stress relaxation function whose effects are added to the stress tensor determined from the Ogden's strain energy function in the FE code [33]. The relaxation function is represented by the Prony series and given by equation (3):

$$g(t) = \sum_{i=1}^{n}\left(G_i e^{-\beta_i t}\right) \quad (3)$$

The parameters of the Prony series (Shear moduli G_i and decay constants β_i) are determined by the code in order to match the input relaxation curve.

Some studies conducted high-strain-rate testing with small liver pieces and reported strong strain rate sensitivity [11-13]. However, these published experiments showed too varied stress-strain curves even if compared with each other at the same strain-rate level to define the rate-dependent property of the liver FE model. Tamura [14] and Nava [34] reported relaxation curves of the liver from time order of 0.1 sec and 1 sec respectively. In the whole liver compression tests, the compression events were done in about 20 sec in the quasi-static loadings described in Step 2 and about 0.006 sec in the dynamic loadings described in the next section, and a relaxation curve from time order of 0.001 sec to 10 sec should be taken into account. Tamura represented the relaxation curve exponentially and Nava showed the initial relaxation modulus in 0.1 MPa order. Therefore, the input relaxation curve shape was estimated based on the literature [14][34] and defined empirically to represent the rate effects obtained from the experiments by simulating a whole liver dynamic compression test described in the next section. Figure 8 shows a comparison of the input relaxation curve with the fitted curve calculated by the code. Table II shows these parameters.

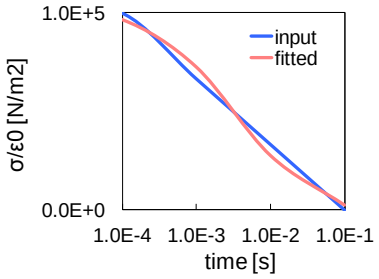

Fig. 8. Relaxation curve in a stress vs. time in logarithmic scale rate-dependent properties

TABLE II
Prony series parameters

i	G_i [Pa]	β_i [-]
1	6.9701E+03	1.0000E+01
2	5.8327E+04	1.0000E+02
3	3.5291E+04	1.0000E+03

Validation of the liver FE model

The liver FE model with the upgraded rate-dependent properties was subjected to a new cycle of validation based on a series of impactor drop tests against whole exsanguinated livers [24] (Test Series 2 in Figure 1 and Figure 9). The impacts were administered with the same type of rigid impactors as those in the quasi-static tests (Figure 10). A total of 20 specimens (10 for the plate, 5 for the cylinder and 5 for the square) were subjected to dynamic load at average impact speed of 3.48 m/s for the plate, 2.84 m/s for the cylinder and 3.37 m/s for the square type up to 60% compression ratio of the initial height. In the frontal impact PMHS sled tests at the velocity of 40 km/h [35], the chest deflection speed caused by a shoulder belt reached around 2 m/s. Therefore this dynamic porcine liver compression experiment targeted the impact velocity of 2 m/s. Because of the limitation of the drop tower testing device, the dynamic compression tests were conducted around 3 m/s.

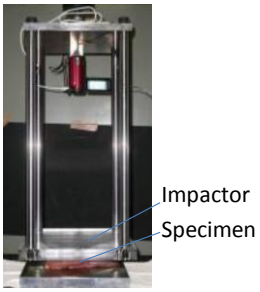

Fig. 9. The drop tower for the dynamic compression tests

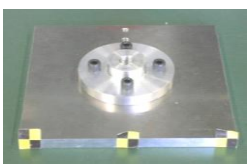

(a) Plate
200 x 200 x 30 mm
Dropping mass: 10.6 kg

(b) Cylinder
ϕ25 x 250 mm
Dropping mass: 9.6 kg

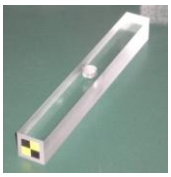

(c) Square
30 x 30 x 250 mm
Dropping mass: 9.7 kg

Fig. 10. Impactors for the dynamic compression test

The experiments were simulated with the liver FE model by administering the average impact speed to each impactor model, and the force compression ratio curves from the simulations were compared with the experimental measurements.

Step 4. Validation of liver tissue ultimate strains from the literature by comparing damaged regions in the simulations with damaged regions in compression tests

Santago [13] reported ultimate strain on hepatic parenchyma at different loading rates under tension and compression (Table A. I). In comparison with the data of that study (Table A. I (a)), the strain rates from our quasi-static compression tests (0.029s-1), which were estimated by the initial height of 35mm (Figure 14 (a)) and loading velocity of 1mm/s, would correspond with values of ultimate strain in compression ranging from -0.61 (Rate 1) to -0.52 (Rate 2). Therefore, either of these two values was implemented in our parenchyma material model as ultimate minimum principle strain. As for dynamic conditions, based on the same data source (Table A. I), an ultimate minimum principle strain of -0.46 was chosen.

As for the hepatic membrane model, a threshold for ultimate maximum principal strain of 0.15 was implemented based on the uni-axial tensile tests of hepatic membrane [23] (Figure A. 1).

With the ultimate strain values implemented in the liver FE model, the model response was investigated by simulating the quasi-static and the dynamic exsanguinated liver tests and by comparing the damaged region and extent of the liver FE model with the damage observed in the corresponding tests.

Step 5. Evaluation of the Applicability of the Liver FE Model to simulate nearly in-vivo conditions

Perfused liver compression tests under quasi-static and dynamic-loading conditions

Two additional series of tests with perfused specimens were conducted [25].The liver of a living subject is filled with blood, which flows inside the organ, affecting its volume when compared with exsanguinated conditions and its response to external loading. In order to approximate in vivo conditions, the specimens were perfused with a constant flow of methylcellulose solution [36] and pressurized with a circulating pump to human and porcine blood pressure level of 130 mmHg [37] (Figure 11).

Quasi-static compression experiments were conducted by using a universal testing machine (AUTOGRAPH, Shimadzu, Kyoto, Japan) (Figure 5) with two types of impactors: plate and cylinder (Figure 12). A total of 10 liver samples (5 for plate and 5 for cylinder type impactors) were subjected to quasi-static load at a velocity of 1mm/s until damage occurred [25] (Test Series 3 in Figure 1).

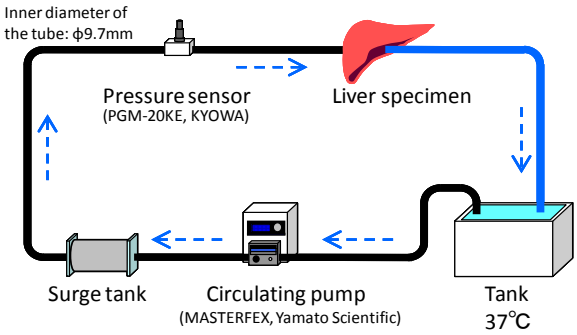

Fig. 11. Schematic diagram of the fluid circulation system

(a) Plate
320 x 320 x 30 mm

(b) Cylinder
ϕ40 x 250 mm

Fig. 12. Impactors for the quasi-static compression test with perfused liver specimens

TABLE III
Test matrix of the perfused porcine liver compression tests under dynamic loadings

Drop height [mm]	Impactor mass [kg]	Impact velocity (Average) [m/s]	Number of test
100	2.5	1.18	3
150	2.0	1.54	5
150	2.25	1.52	8
150	2.5	1.57	5
150	2.75	1.59	3

As for dynamic loading conditions, plate impactor drop tests were conducted by using a drop tower shown in Figure 9 with a plate type impactor (200 x 200 x 20 mm) [25] (Test series 4 in Figure 1). Table III shows the test matrix of the dynamic compression experiment. In order to investigate a threshold for perfused liver damage, the impact energy was controlled by the drop height and impactor mass and set at the level of the occurrence of small damages.

Liver FE model modifications and simulation of tests

The geometry of the liver FE model described in Step 1 (Figure 14 (a)) was employed to match the perfused specimens [25]. 24 porcine liver specimens were measured in length, width and height before and after perfusion (Figure 13). The average size data are listed in Table IV. The liver FE model was scaled up based on the data in Table IV (Figure14). As a first step to estimate liver injury under perfused conditions by using the liver FE model, we attempted to use the liver FE model without modeling the pressure effects to prevent an increase in complexity, and investigated the applicability of the scaled liver FE model in simulating perfused liver conditions.

The scaled liver FE model was subjected to simulations of quasi-static compression tests using perfused whole porcine livers with rigid models of plate and cylinder-type impactors shown in Figure 12 at a velocity of 1 mm/s [25] (Test Series 3 in Figure 1). The scaled liver FE model was also subjected to simulations of dynamic compression tests with plate impactor models at velocities ranging from 1.18 to 1.59 m/s.

By simulating the experiments, the performance of the model to simulate perfused livers could be assessed. In addition, by comparing the strain patterns in the simulations with the damaged regions of the tested specimens, ultimate strains corresponding with nearly in vivo conditions could be estimated.

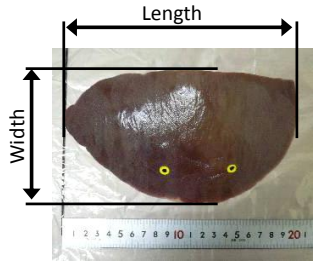

Fig. 13 Measuring the specimen size

TABLE IV
The average size of 24 porcine liver specimen with the standard deviation

	Length [mm]	*Width [mm]*	*Height [mm]*
Exsanguinated	226 (19)	143 (10)	34 (2)
Perfused	242 (22)	153 (11)	74 (9)

(a) Exsanguinated condition
L: 226mm, W:135mm, H:35mm

(b) Perfused condition
L: 242mm, W: 153mm, H 74mm

Fig. 14. Scalling up the liver FE model from exsanguinated condition to perfused condition based on the average size of 24 porcine liver specimens [25]

III. RESULTS

Quasi-static compression response of exsanguinated liver

Figure 15 shows the comparison of force-compression ratio responses in quasi-static tests at a velocity of 1mm/s and their corresponding simulation results with the liver FE model for plate, cylinder and square - type impactors. The experimental results are represented by the average curve ± one standard deviation corridor. The simulation results include the simulated group with ultimate strain values as follows: i) no element elimination, ii) membrane ultimate maximum principal strain of 0.15, iii) membrane ultimate maximum principal strain of 0.15 and parenchyma ultimate minimum principal strain of -0.61, and iv) membrane ultimate maximum principal strain of 0.15 and parenchyma ultimate minimum principal strain of -0.52.

Based on the assumption that liver damage would be associated with a sharp drop in the force-compression ratio curve, the compression ultimate strain defined by minimum principal strain in the liver FE model was validated by comparison of the compression ratio at the time when a sharp drop of force was observed between FEA and experiments. Figure 16 shows an example of sharp force drops in experimental

force-compression ratio curves. The values of the compression ratio at the point of a sharp force drop were extracted, which are summarized in Figure 17 with the average and standard deviation. Results of the FE simulation are also plotted in Figure17.

Figure 18 shows top and lateral images of the specimens after the tests with damaged region in comparison with pictures of the corresponding simulations with regions from which element elimination occurred. To define the damaged internal regions in the experiment, the specimens used in the tests were preserved in formalin after the tests and sliced for visual inspection. The red areas superimposed on pictures of the specimens indicate the damaged internal regions. The dark red areas of the liver FE model indicate eliminated elements in the corresponding simulations.

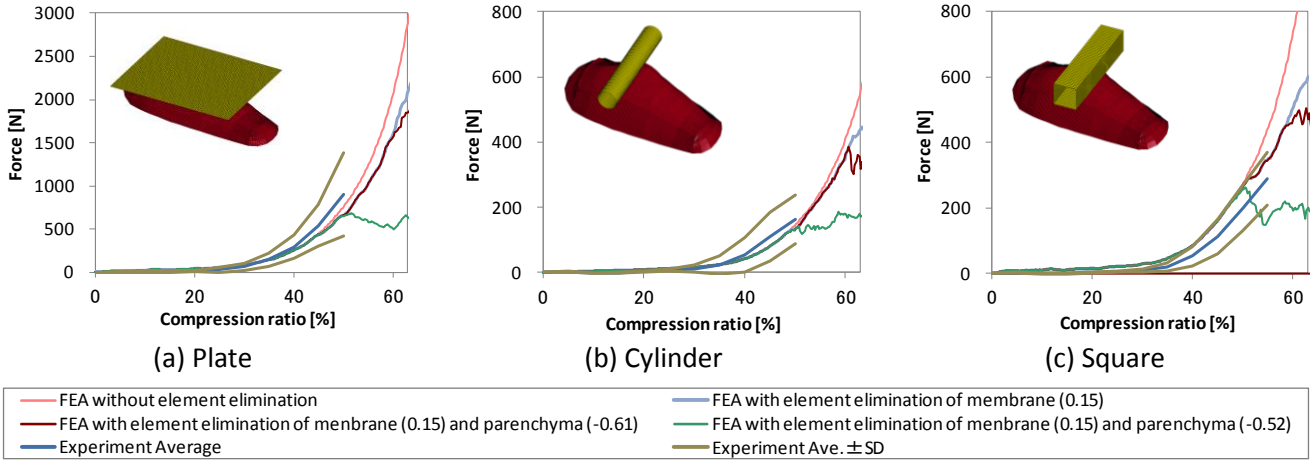

Fig. 15. Force-Compression ratio curves from quasi-static compression tests in comparison to simulated tests for plate (left), cylinder (middle) and square type (right) impactors

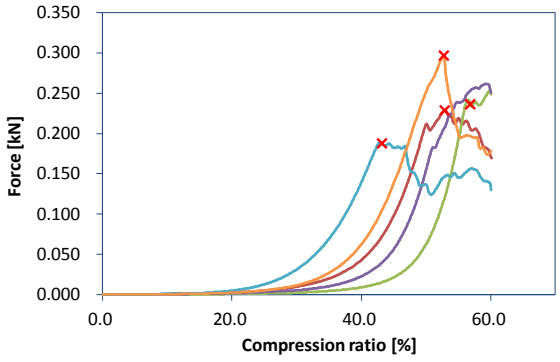

Fig.16. Experimental force compression ratio curves showing damage as a sharp drop caused by tissue damage (quasi-static test with cylindrical impactor)

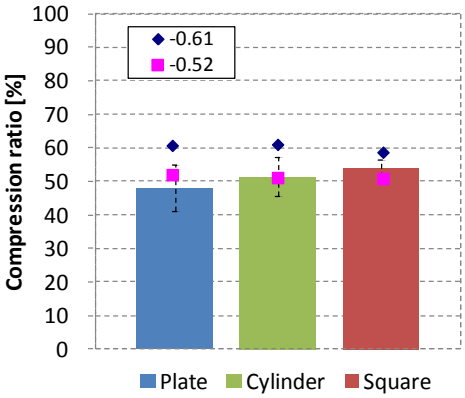

Fig.17. Compression ratio at initiation of tissue damage from the quasi-static tests (Average in colored bars and standard deviation in black lines) and values at which element elimination initiates in the simulations for ultimate strain values of 0.52 (pink square dot) and of 0.61 (blue diamond dot)

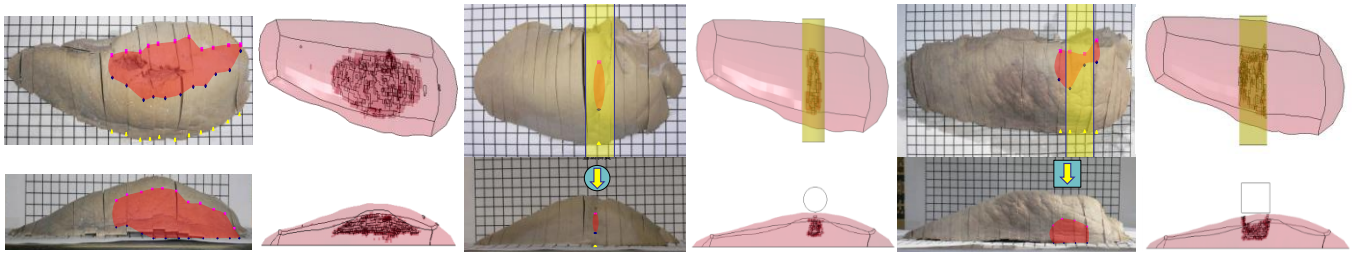

Fig.18. Comparison of damaged regions in the quasi-static compression tests with eliminated regions in the corresponding simulations for plate (left), cylinder (middle) and square (right) type impactors

Dynamic compression response of exsanguinated liver

Figure 19 shows a comparison of force-compression responses in dynamic loading tests with their corresponding simulation results. The experimental results are represented by the average curve ± one standard deviation corridor. The simulation results include the simulated group with ultimate strain values as follows: i) no element elimination and ii) membrane ultimate maximum principal strain of 0.15 and parenchyma ultimate minimum principal strain of -0.46.

A drop of the force in the simulations is detected. However, a sharp force drop could not be captured in the experimental data under dynamic compression as in the quasi-static loading cases. Figure 20 shows top and lateral images of the specimens after the tests with damaged region in comparison with pictures of the corresponding simulations with regions at which element elimination occurred as in Figure 18 in quasi-static cases.

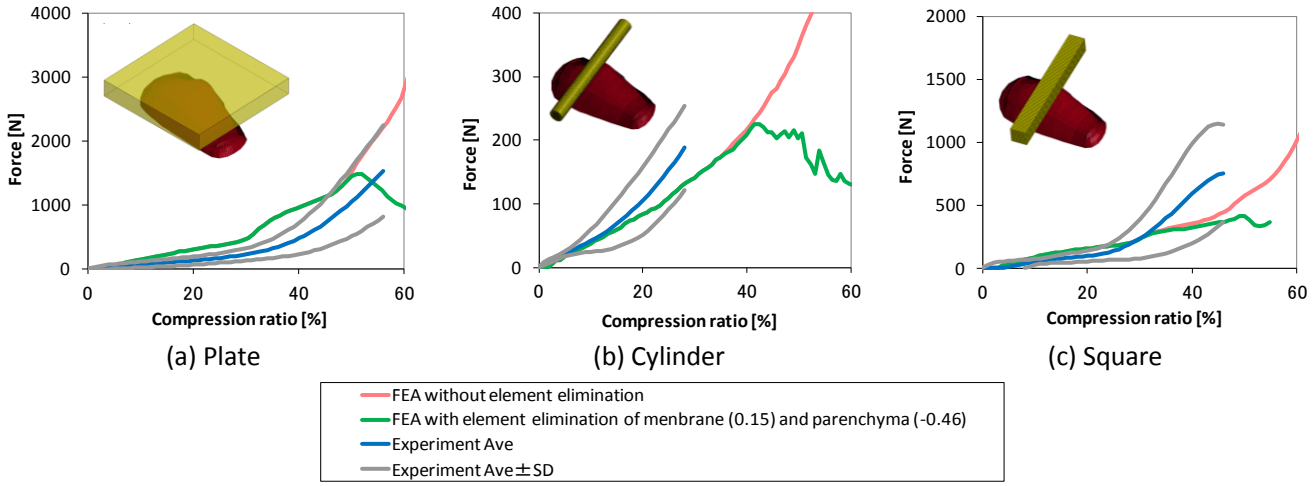

(a) Plate (b) Cylinder (c) Square

Fig.19. Force-Compression ratio curves from dynamic compression tests in comparison to simulated tests for plate (left), cylinder (center) and square (right) type impactors

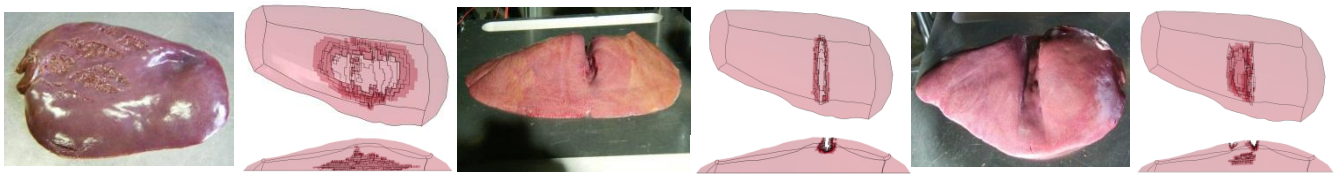

(a) Plate (b) Cylinder (c) Square

Fig.20. Comparison of damaged regions in the dynamic compression tests with eliminated regions in the corresponding simulations at 60% compression ratio of the initial height for plate (left), cylinder (middle) and square (right) type impactors

Quasi-static compression response of perfused liver

Figure 21 shows a comparison of force-compression ratio responses in the quasi-static tests at a velocity of 1mm/s and their corresponding simulation results with the liver FE model for plate and cylinder impactors. The experimental results are represented by the average curve ± one standard deviation corridor. The simulation results include the simulated group with ultimate strain values as follows: i) no element elimination and ii) membrane ultimate maximum principal strain of 0.15 and parenchyma ultimate minimum principal strain of -0.52.

The values of the compression ratio at the point of a sharp force drop were extracted from the experimental data, which are summarized in Figure 22 with the average and standard deviation. Results of the FE simulation are also plotted in Figure 22.

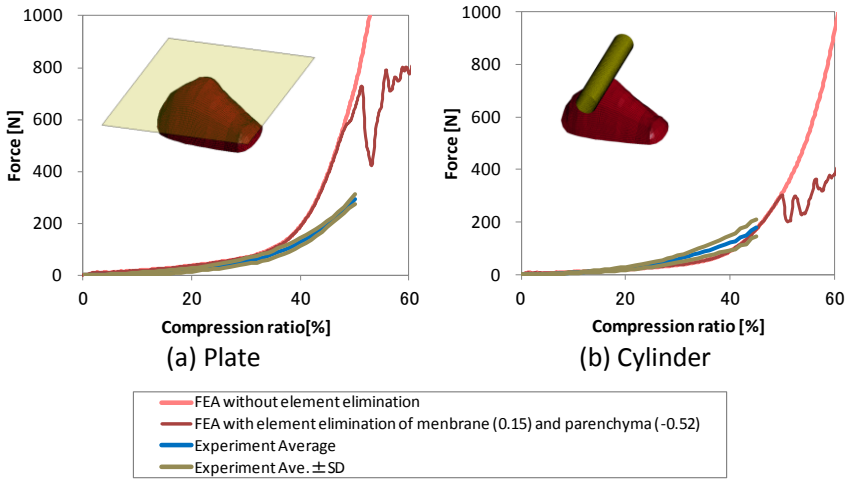

(a) Plate (b) Cylinder

Fig. 21. Force-Compression ratio curves from quasi-static compression tests of perfused liver in comparison to simulated tests for plate (left) and cylinder (right) type impactors

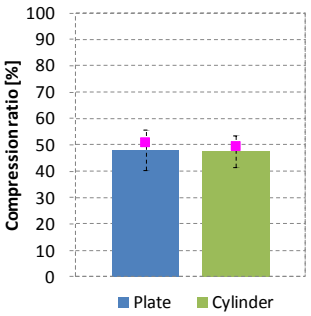

Fig. 22. Compression ratio at initiation of tissue damage from the tests (Average in colored bars and standard deviation in black lines) and values at which element elimination initiates in the simulations for ultimate strain values of 0.52 (pink square dot)

Dynamic compression response of perfused liver

Figure 23 shows a comparison of force-compression responses in the dynamic loading tests with their corresponding simulation results. The experimental results of each test are represented respectively.

Figure 24 shows a comparison of experimental force-compression responses with and without liver damage. This figure explains a tendency that the maximum compression ratios with liver damage are greater than those without liver damage with the experimental data. The maximum compression ratios were extracted, which are summarized in Figure 25. The gray area in Figure 25 indicates a border of the liver damage.

Figure 26 and Figure 27 indicate the liver damage obtained from the experiment. To define the damaged internal regions in the experiment, the specimens used in the tests were preserved in formalin after the tests and sliced for visual inspection. The red areas superimposed on pictures of the specimens indicate the damaged internal regions. Most of the cases with liver damage in Figure 25 have only lacerations on the outer surface as shown in Figure 26. Only one liver sample has parenchyma damage as shown in Figure 27.

Figure 28 shows the true strain distribution of liver membrane at the maximum compression ratio. Figure 29 shows the true strain distribution of liver parenchyma at the maximum compression ratio.

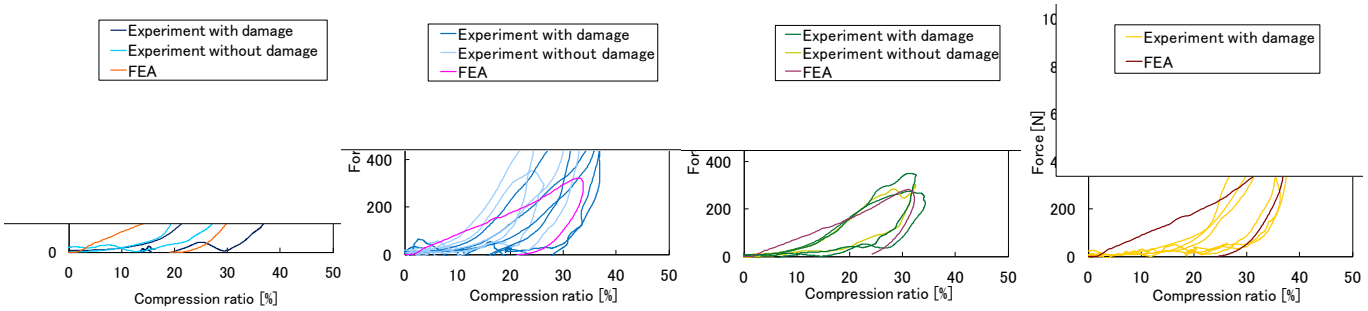

(a) Case: 2kg-1.54m/s (b) Case: 2.25kg-1.52m/s (c) Case: 2.5kg-1.57m/s (d) Case: 2.75kg-1.59m/s

Fig. 23. Force-Compression ratio curves from dynamic compression tests of perfused liver in comparison to simulated tests with drop height of 150mm

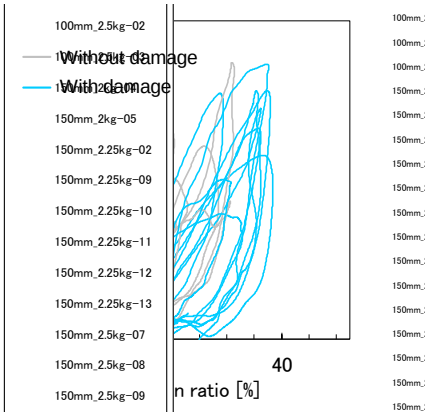

Fig. 24. Experimental Force vs Compression ratio curve with and without liver damage

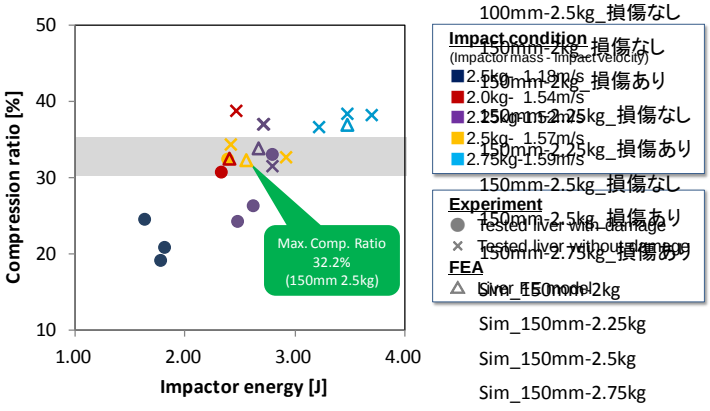

Fig. 25. Maximum compression ratio and occurrence of liver damage

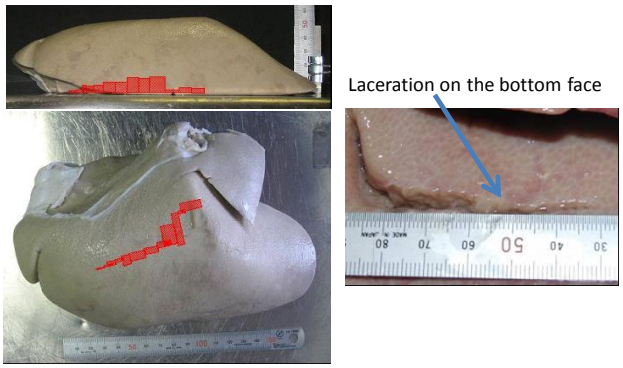

Fig. 26. Liver damage in the Case: 2.5kg-1.57m/s

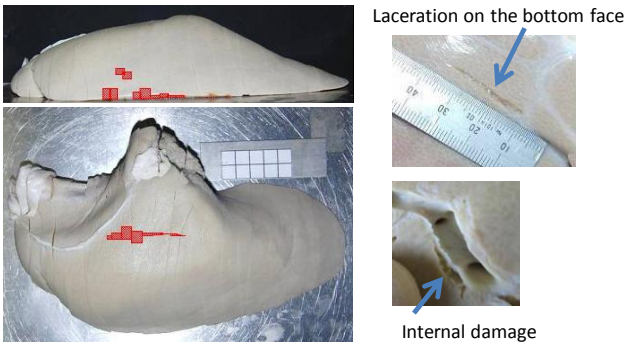

Fig. 27. Liver damage in the Case: 2.75kg-1.59m/s

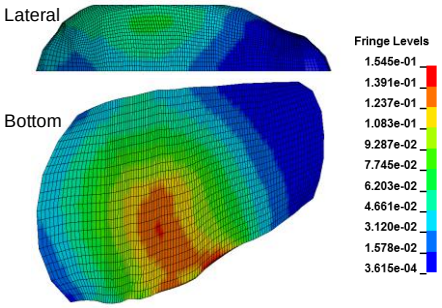

Fig. 28. True Strain distribution of liver membrane at maximum compression ratio without any element elimination definition (Maximum principal strain, Case: 2.5kg-1.57m/s)

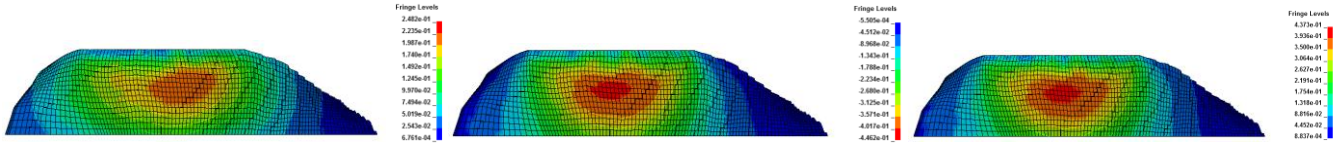

(a) Maximum principal strain (b) Minimum principal strain (c) Effective strain

Fig. 29. True strain distribution of liver parenchyma at maximum compression ratio without any elemen elimination definition (Case: 2.5kg-1.57m/s)

IV. DISCUSSION

Quasi-static compression response of exsanguinated liver

The force-compression curves of the liver FE model under non-perfused quasi-static condition show good agreement with the experimental data (Figure 15). The results of the liver FE model with membrane ultimate strain only show no sharp force drops. These results explain that a sharp force drop on the force-compression ratio curve was derived from parenchyma damage. The compression ratios at the time when a sharp drop of force was observed in the case of the parenchyma ultimate minimum principal strain of -0.52 fall within the range of the experimental average ± one standard deviation (Figure 17). This result corresponds

to the compression ultimate strain reported by Santago. As a result, the ultimate minimum principal strain of hepatic parenchyma is around -0.52 under quasi-static conditions.

Dynamic compression response of exsanguinated liver

In the case of non-perfused dynamic conditions (Figure 20), the force-compression curve of the liver FE model with the plate impactor slightly exceeds the experimental corridor. However, the force-compression curves of the liver FE model with cylindrical and square-type impactors fall within the experimental corridor. A sharp force drop could not be detected in the experiment under dynamic compression when compared between FEA and the experiment such as quasi-static loading. Therefore, the regions where element elimination occurred in the liver FE model were compared with the damaged regions of the specimens after the tests in order to validate the minimum principal strain defined in the parenchyma of the liver FE model. In the square-type impactor, the element elimination region in the perpendicular direction of the bottom surface is around the middle area, but the damaged region of the specimen is around the lower area. On the whole, the element elimination regions of the three types of impactors, however, show the same tendency as those of damaged regions of the specimens. As a result, the ultimate minimum principal strain of hepatic parenchyma could be around -0.46 under dynamic conditions.

Quasi-static compression response of perfused liver

The force-compression curves of the liver FE model under perfused quasi-static conditions show good agreement with the experiment corridor up to the compression ratio of 35% (Figure 21). The differences of the force-compression curve over the compression ratio of 35% between the liver FE model and specimens would be attributed to perfusion. This result indicates that other material models for perfused liver need to be developed if liver behavior is investigated over the compression ratio of 35%. However, such large deformations over the compression ratio of 35% hardly occur under quasi-static conditions when the liver FE model was introduced into the whole human FE model for traffic injury study. Thus, these results explain that the liver FE model validated with non-perfused liver is capable of representing perfused liver compression behavior.

In addition, the compression ratios at the time when a sharp drop of force was observed in the case of the ultimate minimum principal strain of -0.52 fall within the range of the experimental average ± one standard deviation (Figure 22). This result corresponds to the compression ultimate strain reported by Santago [13]. As a result, the ultimate minimum principal strain of perfused hepatic parenchyma is also around -0.52 under quasi-static conditions.

Dynamic compression response of perfused liver

The force-compression curves of the liver FE model under perfused dynamic conditions show a similar tendency with the experimental data and the impactor was rebounded around 35% compression ratio (Figure 23). In the initial stage of compression ratio, the force of the liver FE model increases linearly and is greater than that of experiments. It is because the rate-dependent effects of hepatic parenchyma were modeled as linear viscoelasticity, and because of the limitations of the model. In these cases, the hepatic membrane of the liver FE model had some eliminated elements, but no element eliminations occurred in the parenchyma part of the liver FE model with the ultimate minimum principal strain of -0.46.

Figure 24 explains a tendency that the maximum compression ratios with liver damage are greater than those without liver damage in the experiment. The maximum compression ratios were extracted and are summarized in Figure 25. The gray area in Figure 25 indicates the border of liver damage. The case with the impactor mass of 2.5kg and impact velocity of 1.57m/s was chosen from the gray border, and by comparing the strain patterns in the simulations with the damaged conditions of the tested livers, ultimate strain values to be used for liver FE models of perfused conditions were investigated.

The damage to a tested specimen is shown in Figure 26. The specimen had only lacerations on the outer surface of the bottom area. The maximum principal strain pattern of the membrane elements at the maximum compression ratio also shows strain concentration on the bottom surface (Figure 28). Kaneta [23] conducted the hepatic membrane tension test and reported that the ultimate nominal strain of hepatic membrane was around 15% (0.14% in true strain) as shown in Figure A.1. The red area in Figure 28 indicates the maximum principal strain over 0.14% in true strain and explains the possibility of laceration. On the other hand, the strain distributions of parenchyma shown in Figure 29 have no strain concentrations on the outer area.

Only one liver sample in the case with the impactor mass of 2.75kg and impact velocity of 1.59m/s had small

parenchyma damage as shown in Figure 27 and the damage occurred in the center region. The liver FE model also showed strain concentration in the center region of parenchyma at the maximum compression ratio as shown in Figure 29. Santago [13] reported ultimate strain of hepatic parenchyma at different loading rates under tension and compression (Table A.I). According to that study, the strain rates from our dynamic compression tests (approximately 14s-1) would correspond with the values of ultimate nominal strain in the tension of 0.24 ± 0.07 (Average ± S.D.), ranging from 0.16 to 0.27 in true strain, and in compression of -0.46 ± 0.05, ranging from -0.71 to -0.53 in true strain. In the case of FE simulation with the impactor mass of 2.75kg and impact velocity of 1.59m/s, the maximum value of the maximum principal strain is 0.27 (true strain) is within Santago's ultimate strain corridor in tension. The minimum value of the minimum principal strain is -0.51 (true strain), which is very close to Santago's ultimate strain corridor in compression although it is out of the corridor. The strain value of FE models is affected by its own mesh size, material properties and so on. However these results explain that occurrence of liver injury under perfused conditions could be predicted with the ultimate strain data obtained by fundamental material testings with small piece samples.

Limitations of the study

The liver FE model developed in this study has some limitations as follows: 1) defining the hepatic membrane property as linear elastic, 2) excluding blood pressure or fluid effect modeling, 3) no blood vessel models and 4) using one geometric data set of a lobe. These issues will be addressed in future work to develop a more biofidelic liver FE model to conduct highly reliable injury simulations.

V. CONCLUSIONS

A liver FE model with hyper-viscoelasticity was developed based on exsanguinated liver properties. The applicability of the liver FE model was evaluated against whole perfused porcine liver compression tests under quasi-static and dynamic loadings. The results show that force and displacement of the FE model match the response of perfused livers up to 35% compression ratio. Perfused livers tested under dynamic loading sustained tissue damage in corresponding regions where the FE model showed highest strain concentrations. Based on this correlation, an ultimate strain for hepatic parenchyma and membrane was estimated.

VI. ACKNOWLEDGEMENT

The authors would like to express sincere acknowledgement to the Japan Automobile Manufacturers Association (JAMA) for funding this research.

VII. REFERENCES

[1] Elhagediab AM and Rouhana S, Patterns of abdominal injury in frontal automotive crashes, 16th International ESV Conference Proceedings NHTSA Washinton DC, 1998, pp.770-780.

[2] Rouhana S and Foster, Lateral impact -an analysis of the statistics in the NCSS, Proc. 29th Stapp Car Crash Conference, 1985, pp.79-98.

[3] Hardy W, Investigation of abdominal injury patterns, mechanisms, and tolerances, Proc. 56th Stapp Car Crash Conference, 2012

[4] Melvin J, Stalnaker R and Roberts V et al., 1973, Impact injury mechanisms in abdominal organs, SAE Transactions 730968, pp115-126

[5] Gao Z, Lister K, Desai JP, Constitutive modeling of liver tissue: Experiment and theory, Annals of Biomedical Engineering, 2010, 38(2): 505.

[6] Roan E, Vemaganti K, The nonlinear material properties of liver tissue determined from no-slip uniaxial compression expwriments, Journal of Biomech. Eng., 2007, 129(3): 450-6.

[7] Chui C, Kobayashi E, and Chen X et al., Combined compression and elongation experiments and non-linear modeling of liver tissue for surgical simulation, Medical & Biological Engineering & Computing, 2004, Vol. 42, 787-798.

[8] Sakuma I, Nishimura Y and Chui C et al., In vitro Measurement of Mechanical Properties of Liver Tissue under Compression and Elongation Using a New Test Piece Holding Method with Surgical Glue, Surgery Simulation and Soft Tissue Modeling; Lecture Notes in Computer Science; Vol. 2673, pp 284-292, Springer Berlin Heidelberg, 2003

[9] Fu YB, Chui CK, Teo CL, Liver tissue characterization from uniaxial stress-strain data using probabilistic and inverse finite element methods, Journal of the Mechanical Behavior of Biomedical Materials, 2013 , Volume 20, Pages 105-112.

[10] Umale S, Deck C, and Bourdet N et al., Experimental mechanical characterization of abdominal organs: liver, kidney & spleen, Journal of the Mechanical Behavior of Biomedical Materials, 2013, Volume17, Pages 22-33.

[11] Saraf H, Ramesh KT and Lennon AM et al., Mechanical properties of soft human tissues under dynamic loading, Journal of Biomechanics, 2007, 40, 1960-1967.
[12] Pervin F, Chen W and Weerasooriya T, Dynamic compressive response of bovine liver tissues, Journal of Mechanical Behavior of Biomedical Materials, 2011, 4, 76-84.
[13] Santago AC, Characterizing the biomechanical response of the liver, Master thesis, Virginia Tech, 2010 (http://scholar.lib.vt.edu/theses/available/etd-05142010-101940/unrestricted/Santago_AC_2010.pdf)
[14] Tamura A, Omori K and Miki K et al., Mechanical characterization of porcine abdominal organs, 46th Stapp Car Crash Conference, 2002, 2002-22-0003.
[15] Kerdok AE, Ottensmeyer MP and Howe RD, Effects of perfusion on the viscoelastic characteristics of liver, Journal of Biomechanics, 2006, 39, 2221-2231.
[16] Sparks JL, Bolte IV JH and Dupaix RB et al., Using pressure to predict liver injury tisk from blunt impact, Stapp Car Crash Journal, 2007, 51, 401-432.
[17] Kemper A, Santago A and Sparks J et al., Multi-scale biomechanical characterization of human liver and spleen, Proceedings of the 22nd International Technical Conference on the Enhanced Safety of Vehicles, 2011, Paper number 11-0195.
[18] Kremer MA, Gustafson HM and Bolte IV JH et al., Pressure-based abdominal injury criteria using isolated liver and full-body post-mortem human subject impact tests, Stapp Car Crash Journal, 2011, 55, 317-350.
[19] Jordan P, Socrate S and Zickler TE et al., Constitutive modeling of porcine liver in indentation using 3D ultrasound imaging, Journal of Mechanical Behavior of Biomedical Materials, 2009, 2, 192-201.
[20] Miller K, Constitutive modeling of abdominal organs, Juornal of Biomechanics, 2000, 33, pp367-373.
[21] Snedeker JG, Bajka M and Hug JM et al., The creation of a high-fidelity finite element model of the kidney for use in trauma research, The Journal of Visualization and Computer Animation, 2002, 13, 53-64.
[22] Kim J, An efficient soft tissue characterization algorithm from in vivo indentation experiments for medical simulation, The International Journal of Medical Robotics and Computer Assisted Surgery, 2008, 4, 277-285.
[23] Kaneta Y, Ohkawa H and Suzuki Y et al., Compressive Characteristics of Porcine Whole Liver, J. of Biomechanical Science and Engineering, 2009, Vol. 42, 500-509.
[24] Kaneta Y, Sasahara N and Sato N et al., Quantitative injury evaluation of liver subjected to compressive loading, M&M2010, 2010, No. 1309.
[25] Sato N, Hara T and Yamamoto Y et al., The injury mechanism of perfusion liver in the quasi-static compression experiments, Biofronteer JSME, 2009, A117.
[26] Takahashi M, Ogi K and Tanaka D et al., Mechanical properties pf the liver under compression loading, Trans. Jpn. Soc. Mech. Eng, 2005, A71-702, 353-358.
[27] Brunon A, Bruyere-Garnier K and Coret M, Mechanical characterization of liver capsule through uniaxial quasi-static tensile tests until failure, Journal of Biomechanics, 2010, 43, 2221-2227.
[28] Brunon A, Bruyere-Garnier K and Coret M, Characterization of the nonlinear behaviour and the failure of human liver capsule through inflation tests, Journal of the Mechanical Behavior of Biomedical Materials, 2011, 4, 1572-1581.
[29] Ogden RW, Large deformation isotropic elasticity -on the correlation of theory and experiment for incompressible rubberlike solids, Proc. R. Soc. Lond. A. 326, 1972, 565-584
[30] Fung YC, Biomechanics: Mechanical properties of living tissue, Springer, New York, 1993
[31] Farshad M et al., Material characterization of the pig kidney in relation with the biomechanical analysis of renal trauma, Journal of Biomechanics, 1999, 32, 417-425.
[32] Mendis KK et al., A constitutive relationship for large deformation finite element modelling of brain tissue, Journal of Biomechanical Engineering, 1995, 117, 279-285.
[33] Hallquist, LS-DYNA Theory Manual, Livemore Software Technology Corporation, California, 2006.
[34] Nava A, Mazza E and Kleinermann F et al., Determination of the mechanical properties of soft human tissues through aspiration experiments, Lecture Notes in Computer Science, 2003, Vol. 2878/2003, 222-229.
[35] Shaw G, Parent D and Purtsezov S et al., Frontal impact PMHS sled tests for torso model development, IRCOBI, 2009.
[36] Iida R, Quantitative investigation of depredation by blood flow induced mechanical stress: development of in vitro evaluation system of blood vessel depredatio, JSME 17th Biofrontier Symposium, 2006, pp53-54.
[37] Tajima Y, Biological Reference Data Book on Experimental Animals, Soft Science, Tokyo, 1989.

VIII. APPENDIX

TABLE A. I Failure strain of liver parenchyma from Santago 2010 [13]

(a) compression

Rate	Desired Strain Rate [s^{-1}]	No. of tests	Average	
			Strain Rate [s^{-1}]	Failure Strain (Nominal strain)
Rate 1	0.007	9	0.008±0.001	-0.61±0.05
Rate 2	0.070	9	0.074±0.001	-0.52±0.04
Rate 3	0.700	9	0.776±0.104	-0.46±0.05
Rate 4	7.000	9	8.011±0.834	-0.46±0.05

(b) Tension

Rate	Desired Strain Rate [s^{-1}]	No. of tests	Average	
			Strain Rate [s^{-1}]	Failure Strain (Nominal strain)
Rate 1	0.01	16	0.008±0.001	0.34±0.12
Rate 2	0.10	11	0.089±0.001	0.32±0.05
Rate 3	1.00	12	0.871±0.104	0.30±0.10
Rate 4	10.00	12	9.524±0.834	0.24±0.07

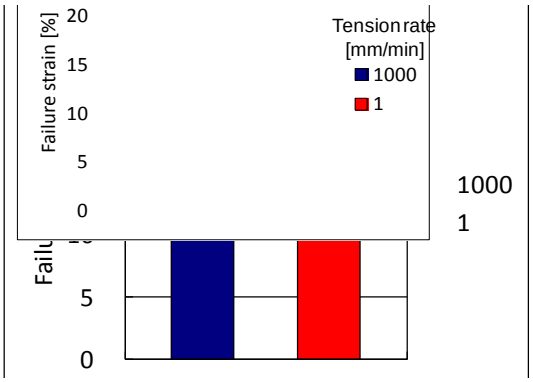

Fig. A.1. Failure strain of liver membrane obtained from tensile tests by Kaneta et al. [23]